Nuclear Instruments and Methods in Physics Research B 404 (2017) 264–268

Contents lists available at ScienceDirect

Nuclear Instruments and Methods in Physics Research B

journal homepage: www.elsevier.com/locate/nimb

Nuclear microprobe investigation of the effects of ionization and displacement damage in vertical, high voltage GaN diodes

G. Vizkelethy [a,*], M.P. King [a], O. Aktas [b], I.C. Kizilyalli [b,1], R.J. Kaplar [a]

[a] Sandia National Laboratories,[2] Albuquerque, NM, USA
[b] Avogy, Inc., San Jose, CA, USA

ARTICLE INFO

Article history:
Received 9 August 2016
Received in revised form 24 October 2016
Accepted 24 November 2016
Available online 2 December 2016

Keywords:
GaN
IBIC
Displacement damage

ABSTRACT

Radiation responses of high-voltage, vertical gallium-nitride (GaN) diodes were investigated using Sandia National Laboratories' nuclear microprobe. Effects of the ionization and the displacement damage were studied using various ion beams. We found that the devices show avalanche effect for heavy ions operated under bias well below the breakdown voltage. The displacement damage experiments showed a surprising effect for moderate damage: the charge collection efficiency demonstrated an increase instead of a decrease for higher bias voltages.

1. Introduction

Power electronics are used in many fields ranging from computer to auto industry, from terrestrial to space applications. Traditional Si-based power electronics went through huge progress, becoming smaller and more efficient over time. As requirements are constantly pushing for more and more performance improvement, the same Si-based devices are reaching their fundamental material limitations [1–3]. Wide bandgap materials such as SiC and GaN allow further improvements in power efficiency, size, and weight making them an attractive alternative to conventional Si-based power devices. The large bandgap (3.4 eV) and high breakdown field (>3 MV/cm) of GaN-based power devices [4] give a unipolar figure of merit (turn-on resistance vs. breakdown voltage) that not only exceeds that of Si, but is even better than that of SiC. Until recently, the lack of high quality, native substrates for GaN forced device manufacturers to use Si, SiC, and sapphire substrates. This led to high threading dislocation density in the devices [5], which caused poor performance and reliability issues. Recently, suitable high quality substrates became available on the market. In this paper we investigate the radiation response of vertical, high-voltage, GaN diodes on high quality bulk GaN substrate.

Electronic devices are exposed to harsh radiation environment from space to nuclear reactors and high-energy particle colliders. Radiation generally interacts in solids with both the electrons (ionization) and lattice atoms (displacement damage). Ionization primarily impacts transistors causing transient currents and deleterious circuit-level effects; such as a bit flip in an SRAM cell. In diodes the ionization can lead to enhanced charge collection through impact ionization, and in some cases when the current is not limited, avalanche processes can cause single event burnout (SEB) [6,7].

Displacement damage creates lattice defects with states in the bandgap, which lowers carrier lifetime and increases recombination. This in turn increases leakage current, lowers breakdown voltage, and if the diode is used as a radiation detector, its charge collection efficiency will diminish. There are several methods to measure the effect of displacement damage, such as *C-V* measurements to determine carrier compensation or Deep Level Transient Spectroscopy (DLTS) [8] to identify types and concentration of the defects. These are bulk techniques, the entire device needs to be irradiated and even with low fluences the leakage current can become too high to prohibit using the above techniques. In addition, if fluence dependence has to be measured, either many devices have to be used or one has to go through several irradiation-measurement cycles, which can take a long time. Ion Beam Induced Charge [9] (IBIC) and Time Resolved IBIC [10,11] (TRIBIC) measure the damage locally. Using a nuclear microprobe small areas can be irradiated and the local change in Charge Collec-

* Corresponding author.
E-mail address: gvizkel@sandia.gov (G. Vizkelethy).

[1] I.C. Kizilyalli currently is with Advanced Research Project Agency – Energy, US DOE, 1000 Independence Ave. SW, Washington, DC 20585.

[2] Sandia National Laboratories is a multi-program laboratory managed and operated by Sandia Corporation, a wholly owned subsidiary of Lockheed Martin Corporation, for the U.S. Department of Energy's National Nuclear Security Administration under contract DE-AC04-94AL85000.

http://dx.doi.org/10.1016/j.nimb.2016.11.031
0168-583X/

tion Efficiency (CCE) can be measured. This will give an indication of displacement damage. Using this approach, one device can be irradiated with many fluences and the localized response compared. IBIC [12,13], Electron Induced Current (EBIC) [12], and scanning photocurrent microscopy [14] were used in the past to characterize electric fields in high power diodes (not the ones in this paper) to understand the effects of edge termination. We used IBIC to investigate the effects of edge termination guard rings in these diodes.

2. Experimental

The diodes used in this experiment have been described in detail elsewhere [4,15,16]. The same types of devices were used to study displacement damage using broad beam irradiation by 2.5 MeV protons [17]. Fig. 1 shows the schematic of the device [4]. C-V measurements were performed to determine the doping level of the n- layer and the depletion width dependence on the bias voltage. The doping was measured to be $\sim 10^{16}$ dopant/cm^3 and the device became fully depleted to 10 μm between 800 and 1000 V depending on device. All the devices exhibited a non-destructive breakdown around 1700 V. The devices in addition to the front electrode had guard rings at the edges to improve the breakdown performance. Four ion-energy combinations were used, 1 MeV H, 3.8 MeV He, 25 MeV O, and 45 MeV Si. The energies were selected in such a way that the end-of-range damage peak was at 6 μm depth. The ionization profile was almost entirely between the surface and the damage peak. Since the diodes' front surface was biased negative, the electrons had to go through the highly damaged region and a very small fraction of holes that are generated inside the damaged region in the tail of the ionization profile. The ion beams were focused to about 1 μm. CCE bias curves were measured up to 1000 V scanning the ion beams on a large area to avoid damage. For the damage measurements a small, typically 50×50 μm^2 area was used and the IBIC signal was taken from the center 25×25 μm^2 area to avoid edge effects [18]. The damage was measured by the IBIC signal from the damaging ion (continuous fluence measurement). In addition, small areas were irradiated with the heavy ions (O and Si) at low bias to measure the fluence and were measured with light ions at different bias voltages.

The IBIC measurements were performed using an Ortec 142A preamplifier, Ortec 671 spectroscopy amplifier, and an MPA3 multi-parameter system measurement chain. The IBIC signal was calibrated using a Hamamatsu S1223 photo diode taking into account the difference between energies needed to create an electron-hole pair in Si (3.62 eV) and in GaN (8.9 eV) [19,20]. A few TRIBIC signals were recorded using a Tektronix DPO 72004 digital oscilloscope with 20 GHz analog bandwidth and 50 GSamples/s sampling rate.

3. Results

Fig. 2 shows the CCE dependence on the applied bias. Since the hole carrier lifetime is very short in this material, we can use a simple model to calculate the CCE (holes that would diffuse to the depletion layer will recombine). The CCE as a function of applied bias is:

$$CCE(V) = \frac{\int_0^{w(V)} S_e(x)dx}{E_{ionization}} \quad (1)$$

where V is the applied bias, w is the depletion depth as the function of applied bias, $S_e(x)$ is the ionization profile calculated from SRIM [21], and $E_{ionization}$ is the total energy going into ionization. As mentioned above, the ionization profile extends to about

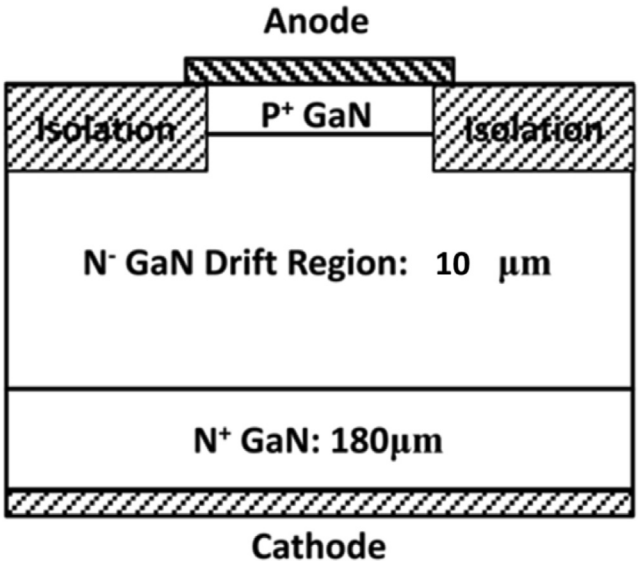

Fig. 1. Schematic view of the vertical GaN diode. The edge termination rings are not shown.

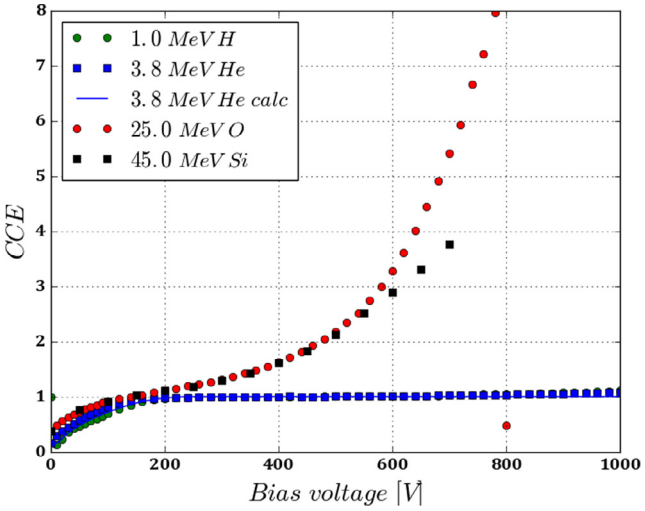

Fig. 2. Charge collection efficiency as the function of applied bias. The H and He curves and the He simulation curves are practically the same.

6 μm from the surface for each ion/energy combination. The depletion depth becomes 6 μm around 200 V; therefore, we can expect 100% CCE above 200 V. As Fig. 2 shows this is the case for the light ions. The heavy ions' CCE exceeds 100% above 200 V and is rapidly increasing. Although the breakdown voltage of each device was above 1700 V, the devices irradiated with the heavy ions suffered a destructive breakdown at 700–900 V. The breakdown manifested itself in various forms. In most cases the diode became a short, in other cases its leakage current increased by 6–7 orders of magnitude. In some cases, even physical damage (burn marks on the top electrode) could be observed. Under heavy ion irradiation the devices undergo avalanche due to impact ionization and charge multiplication is observed. If someone examines a bit more closely the H and He CCE curves, it is obvious that the same phenomenon starts to happen above 900 V, although to much less extent (<20% increase in CCE). The avalanche is obvious from the TRIBIC measurement, too. Fig. 3 shows the ion beam induced current from 45 MeV Si ions at three bias voltages. The ringing is due to poor impedance matching to the 50 Ω input impedance of the oscilloscope. According to the Gunn theorem, the induced current is

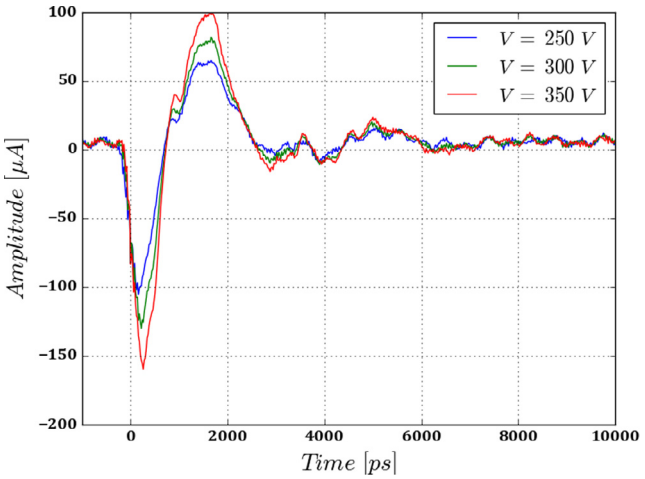

Fig. 3. Average of around four hundred single current transients form 45 MeV Si ions at different bias voltages. Transients below the 250 V were too small to detect. At these voltages the transients are clearly due to avalanches.

$$i = -q \cdot \vec{v}_d \cdot \frac{\partial \vec{E}}{\partial V} \tag{2}$$

For a diode the partial differential in (1.2) is constant, $1/w$ [22], so the induced current is proportional to the carrier drift velocity. The widths of the signals are the same, which means that the transit time of the carriers does not depend on the bias. That would be the case if the drift velocities of the carriers were saturated even at the lowest bias. TCAD calculations showed that it is the actual case, the drift velocities are the same at 250 V and 350 V. The discussion of these calculations is outside of the scope of the paper, but details can be found in [23] for a similar device. In this case if the charge induction was normal, the maximum currents should be the same, too. We can observe that the maximum current is increasing with increasing electric field, as it should for an avalanche.

Fig. 4 shows the in-situ damage measurement at various bias voltages with the 3.8 MeV He (a) and 25 MeV O (b) beams. The expectation is that the CCE decreases with increasing fluence due to the increased recombination (which also means decreased lifetime). The He CCE curves follow the expectation (except at 500 V where a small increase can be observed) but for O above ~300 V the CCE increases at first before it starts to decrease. This shows

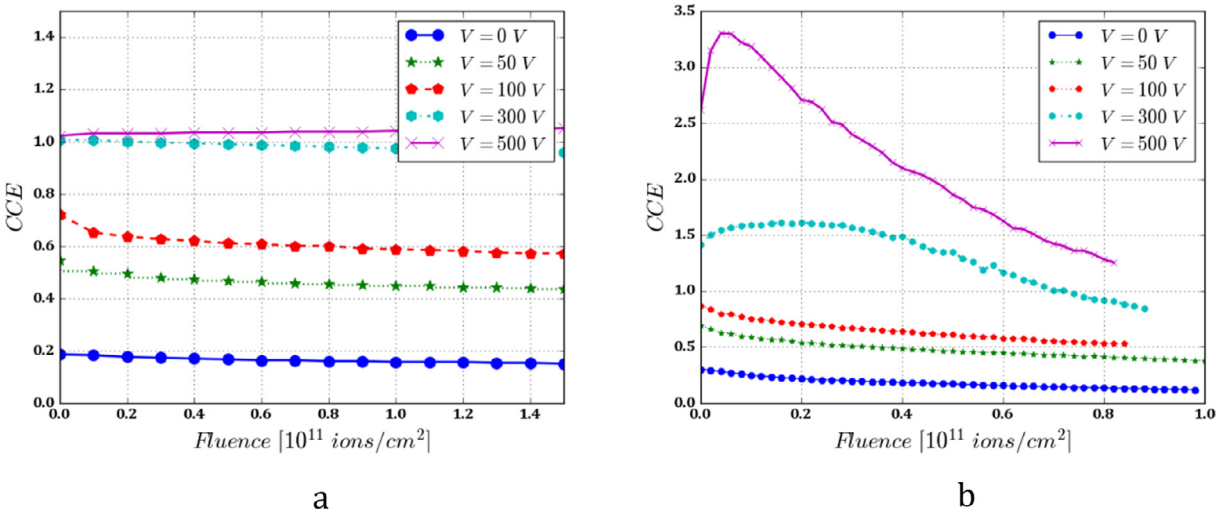

Fig. 4. CCE as the function of the fluence, (a) 3.8 MeV He and (b) 25 MeV O.

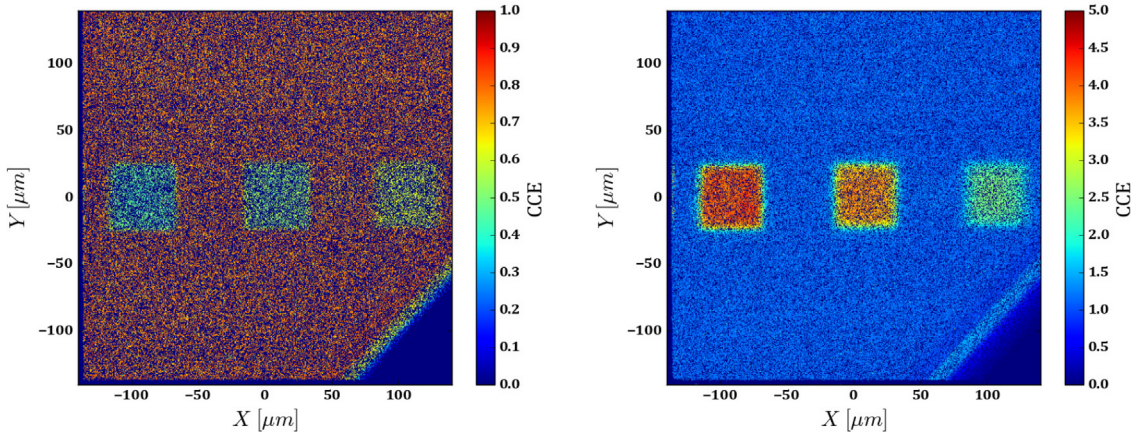

Fig. 5. CCE maps of spots irradiated with different fluences (a) at 100 V, (b) at 1000 V. The fluences are from right to left 5.5×10^9, 1.09×10^{10}, and 1.61×10^{10} ions/cm^2. The irradiations were done with 45 MeV Si ions, the IBIC measurement was done with 3.8 MeV He ions.

that using the same heavy ion to measure the damage is not really feasible. A light ion such as H or He should be used.

One device was irradiated at six different fluence levels with 45 MeV Si ions and bias curves were measured with 3.8 MeV He. Since there was no avalanche with the He beam we expected normal CCE vs. fluence curves at all biases. Fig. 5 shows the CCE maps of the three lowest fluences at 100 V and 1000 V bias. The fluence is increasing from the right to the left. Fig. 6 shows the cross section along the middle of the irradiated spots. It is clear that avalanche is occurring with the He beam, more damage results in higher charge multiplication. At the lower bias the effect is as expected, CCE is monotonically decreases with increasing fluence. At higher voltages the CCE is monotonically increasing with increasing fluence up to a certain level when it starts decreasing, behaving as expected. At this point we just speculate what the mechanism might be. Defects are usually at midgap, at least the ones that are the most effective recombination centers. They serve as compensating and recombination centers normally, decreasing the background doping, carrier lifetime, and CCE. The impact ionization that leads to avalanche moves electrons from the valence band to the conduction band. But in a device with defects there are electrons and holes captured by the defects. Since they are at midgap it takes less energy to raise them to the conduction band; therefore, there will be more carriers per unit energy particularly if the number of defects is on the same order of magnitude (or higher) as the intended doping concentration. The carriers from the ionized defects raise the normally low density to high enough to initiate an avalanche. Another explanation can be that the trapped carriers in the defects increase the local electric field above the limit for charge multiplication. As we saw above, the avalanche depends on the e-h plasma density, and possibly occurs above some threshold carrier density and electric field. At some point the decreased lifetime will overcome this effect and the CCE will start decreasing. Fig. 7 shows the CCE vs. bias curves for different fluences with 45 MeV Si creating damage and 3.8 MeV He measuring CCE. To avoid clutter the individual curves are not labeled but they increase from 0 V to 1000 V. Below a certain bias voltage (~500 V) there is no avalanche, the CCE decreases. Above that all the curves exhibit an increasing CCE, then start decreasing above the fluence of 1.6×10^{10} ions/cm^2. Similar effect was recently found in AlGaN/GaN HEMTs (High Electron Mobility Transistor) irradiated with 2 MeV protons at the fluence of 6×10^{14} protons/cm^2 [24]. Furthermore, this effect was observed in silicon [25,26] and diamond [27] detectors recently.

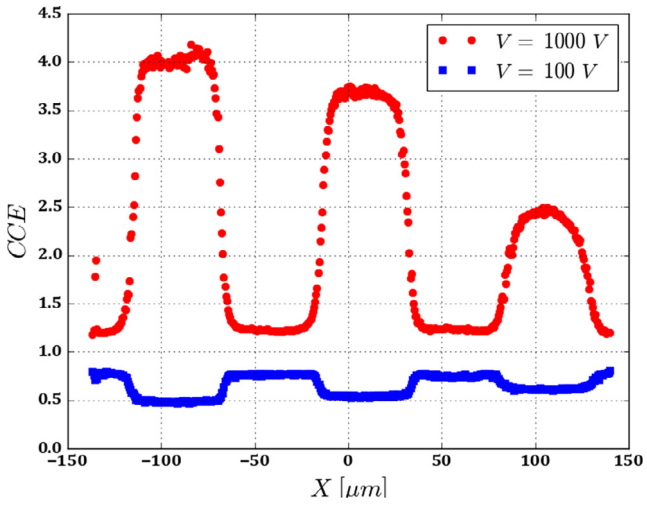

Fig. 6. Cross section in the X direction from Fig. 5.

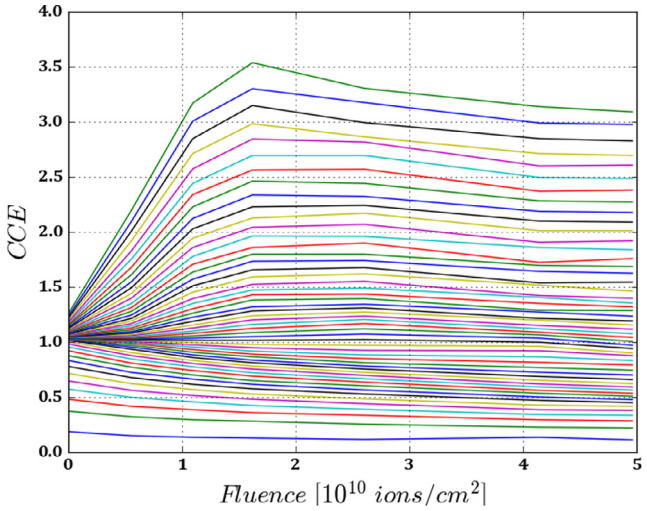

Fig. 7. CCE dependence on fluence at bias voltages from 0 to 1000 V by 20 V steps. The voltage increases from the bottom to the top.

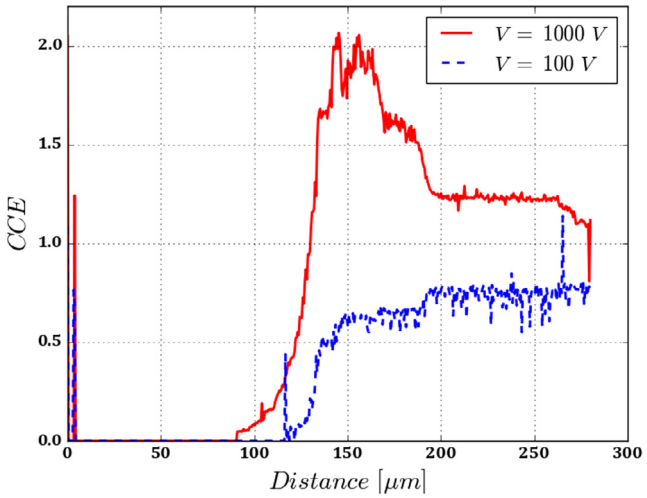

Fig. 8. IBIC line scan over the edge termination area at 100 and 1000 V bias. The anode starts around 200 μm and extends to the right.

The effect of the edge termination was briefly investigated using 3.8 MeV He IBIC. The beam was scanned along a line over the edge termination rings and part of the anode electrode at various bias voltages. For clarity we show only the scans at 100 V and 1000 V in Fig. 8. The anode electrode starts at around 200 μm and extends toward the right. The edge of the devices is around 120 μm and the edge termination rings extend to about 170 μm. The rest between the anode electrode and the rings is the isolation. Over the anode the CCE starts out around 50% and at 1000 V exceeds unity by about 20%. This is what was previously observed on undamaged devices. However the CCE increases well above 2 over the edge terminations, and even over the insulator area it exceeds the CEE in the anode area. This indicates avalanches in these areas, due to much higher electric fields than under the anode electrode. In these areas the electric field exceeds the threshold for avalanches for the 3.8 MeV He beam.

4. Conclusions

The radiation response of high-voltage, vertical GaN diodes was investigated. We found that although the non-radiation break-

down of these diodes was above 1700 V, heavy ion (25 MeV O and 45 MeV Si) irradiations triggered carrier multiplication by impact ionization processes at as low as 200 V, which at higher voltages led to destructive breakdown of the devices. The effect showed a very strong dependence on the e-h plasma density. For light ions (H, He) with ionization energy loss in the order of tens of eV/Å no avalanches were initiated until above 1000 V. The heavy ions had hundreds of eV/Å energy loss, which led to impact ionization at low voltages.

The CCE measurements of damaged devices led to an interesting observation. At higher voltages where the end-of-range damage peak fell into the depletion layer at moderate damage the CCE was enhanced and charge multiplication was observed even with the light ion beams. The charge multiplication increased with increasing damage up to a point when it was reversed. We speculate that this enhancement is due to the fact that carriers can ionize the defects in the bandgap more easily than from the valance band. That probably can increase the e-h plasma density to reach the avalanche threshold. As the damage increases more defects will be available for ionization so the charge multiplication increases. Eventually, the increased recombination and decreased lifetime dominate the response and the CCE starts decreasing with additional damage.

The effect of edge termination was investigated. We found that while the electric field/e-h plasma density does not cause significant avalanche for light ion irradiation under the anode electrode, the electric field exceeds the threshold under the edge termination and insulation areas, triggering avalanches.

References

[1] B.J. Baliga, Power semiconductor-device figure of merit for high-frequency applications, IEEE Electron Device Lett. 10 (1989) 455–457.
[2] B.J. Baliga, Trends in power semiconductor devices, IEEE Trans. Electron Devices 43 (1996) 1717–1731.
[3] B.J. Baliga, Gallium nitride devices for power electronic applications, Semicond. Sci. Technol. 28 (2013).
[4] I.C. Kizilyalli, A.P. Edwards, O. Aktas, T. Prunty, D. Bour, Vertical Power p-n Diodes Based on Bulk GaN, IEEE Trans. Electron Devices 62 (2015) 414–422.
[5] T.J. Anderson, M.J. Tadjer, J.K. Hite, J.D. Greenlee, A.D. Koehler, K.D. Hobart, F.J. Kub, Effect of reduced extended defect density in MOCVD grown AlGaN/GaN HEMTs on native GaN substrates, IEEE Electron Device Lett. 37 (2016) 28–30.
[6] A.M. Albadri, R.D. Schrimpf, K.F. Galloway, D.G. Walker, Single event burnout in power diodes: mechanisms and models, Microelectron. Reliab. 46 (2006) 317–325.
[7] K.H. Maier, A. Denker, P. Voss, H.W. Becker, Single event burnout of high-power diodes, Nucl. Instrum. Methods Phys. Res. Sect. B 146 (1998) 596–600.
[8] D.V. Lang, Deep-level transient spectroscopy- new method to characterize traps in semiconductors, J. Appl. Phys. 45 (1974) 3023–3032.
[9] M.B.H. Breese, E. Vittone, G. Vizkelethy, P.J. Sellin, A review of ion beam induced charge microscopy, Nucl. Instrum. Methods Phys. Res. Sect. B 264 (2007) 345–360.
[10] H. Schone, D.S. Walsh, F.W. Sexton, B.L. Doyle, P.E. Dodd, J.F. Aurand, R.S. Flores, N. Wing, Time-resolved ion beam induced charge collection (TRIBICC) in micro-electronics, IEEE Trans. Nucl. Sci. 45 (1998) 2544–2549.
[11] N. Schone, D.S. Walsh, F.W. Sexton, B.L. Doyle, P.E. Dodd, J.F. Aurand, N. Wing, Time-resolved ion beam induced charge collection (TRIBICC) in micro-electronics, Nucl. Instrum. Methods Phys. Res. Sect. B 158 (1999) 424–431.
[12] R. Siemieniec, A. Pugatschow, C. Geissler, H.J. Schulze, F.J. Niedernostheide, R. Heiderhoff, L.J. Balk, Analysis of power devices breakdown behaviour by ion beam and electron beam induced charge microscopy, in: 9th International Seminar on Power Semiconductors, ISPS'08, Prague, Chech Republic, 2008, pp. 201–207.
[13] M. Zmeck, L.J. Balk, R. Heiderhoff, T. Osipowicz, F. Watt, J.C.H. Phang, A.M. Khambadkone, F.J. Niedernostheide, H.J. Schulz, Analysis of E-field distributions within high-power devices using IBIC microscopy, in: Proceedings of the 17th International Symposium on Power Semiconductor Devices & Ics, Santa Barbara, CA, 2005, pp. 235–238.
[14] F. Lèonard, J.R. Dickerson, M.P. King, A.M. Armstrong, A.J. Fischer, A.A. Allerman, R.J. Kaplar, A.A. Talin, In-operando spatial imaging of edge termination electric fields in GaN vertical p-n junction diodes, IEEE Electron Device Lett. 37 (2016) 766–769.
[15] O. Aktas, I.C. Kizilyalli, Avalanche capability of vertical GaN p-n junctions on bulk GaN substrates, IEEE Electron Device Lett. 36 (2015) 890–892.
[16] I.C. Kizilyalli, A.P. Edwards, H. Nie, D. Disney, D. Bour, High voltage vertical GaN p-n diodes with avalanche capability, IEEE Trans. Electron Devices 60 (2013) 3067–3070.
[17] M.P. King, A.M. Armstrong, J.R. Dickerson, G. Vizkelethy, R.M. Fleming, J. Campbell, W.R. Wampler, I.C. Kizilyalli, D.P. Bour, O. Aktas, H. Nie, D. Disney, J. Wierer, A.A. Allerman, M.W. Moseley, F. Leonard, A.A. Talin, R.J. Kaplar, Performance and breakdown characteristics of irradiated vertical power GaN P-i-N diodes, IEEE Trans. Nucl. Sci. 62 (2015) 2912–2918.
[18] B.L. Doyle, G. Vizkelethy, D.S. Walsh, Ion beam induced charge collection (IBICC) studies of cadmium zinc telluride (CZT) radiation detectors, Nucl. Instrum. Methods Phys. Res. Sect. B 161 (2000) 457–461.
[19] A. Owens, A. Barnes, R.A. Farley, M. Germain, P.J. Sellin, GaN detector development for particle and X-ray detection, Nucl. Instrum. Methods Phys. Res. Sect. A 695 (2012) 303–305.
[20] J. Wang, P.L. Mulligan, L.R. Cao, Transient current analysis of a GaN radiation detector by TCAD, Nucl. Instrum. Methods Phys. Res. Sect. A 761 (2014) 7–12.
[21] J.F. Ziegler, SRIM, <http://www.srim.org/>, 2008.
[22] E. Vittone, Theory of ion beam induced charge measurement in semiconductor devices based on the Gunn's theorem, Nucl. Instrum. Methods Phys. Res. Sect. B 219-20 (2004) 1043–1050.
[23] J.R. Dickerson, A.A. Allerman, B.N. Bryant, A.J. Fischer, M.P. King, M.W. Moseley, A.M. Armstrong, R.J. Kaplar, I.C. Kizilyalli, O. Aktas, J.J. Wierer Jr., Vertical GaN power diodes with a bilayer edge termination, IEEE Trans. Electron Devices 63 (2016) 419–425.
[24] A. Khachatrian, N.J.-H. Roche, S.P. Buchner, A.D. Koehler, J.D. Greenlee, T.J. Anderson, J.H. Warner, D. McMorrow, Spatial mapping of prisitine and irradiated AlGaN/GaN HEMTs with UV single-photon absorption single-event transient technique, IEEE Trans. Nucl. Sci. (2016).
[25] G. Casse, A. Affolder, P.P. Allport, H. Brown, M. Wormald, Enhanced efficiency of segmented silicon detectors of different thicknesses after proton irradiations up to $1 \times 10(16)$ n(eq) cm(2), Nucl. Instrum. Methods Phys. Res. Sect. A 624 (2010) 401–404.
[26] G. Casse, D. Forshaw, T. Huse, I. Tsurin, M. Wormald, M. Lozano, G. Pellegrini, Charge multiplication in irradiated segmented silicon detectors with special strip processing, Nucl. Instrum. Methods Phys. Res. Sect. A 699 (2013) 9–13.
[27] N. Skukan, Personal communication, 2016.